


A novel 3-oxoacyl-ACP reductase (FabG3) is involved in the xanthomonadin biosynthesis of *Xanthomonas campestris* pv. *campestris*

YONGHONG YU ^{1,2}, JIANRONG MA¹, QIAOQIAO GUO², JINCHENG MA² AND HAIHONG WANG^{2,*}

¹Guangdong Food and Drug Vocational College, Guangzhou, Guangdong 510520, China

²Guangdong Provincial Key Laboratory of Protein Function and Regulation in Agricultural Organisms, College of Life Sciences, South China Agricultural University, Guangzhou, Guangdong 510642, China

SUMMARY

Xanthomonas campestris pv. *campestris* (*Xcc*), the causal agent of black rot in crucifers, produces a membrane-bound yellow pigment called xanthomonadin to protect against photobiological and peroxidative damage, and uses a quorum-sensing mechanism mediated by the diffusible signal factor (DSF) family signals to regulate virulence factors production. The *Xcc* gene XCC4003, annotated as *Xcc fabG3*, is located in the *pig* cluster, which may be responsible for xanthomonadin synthesis. We report that *fabG3* expression restored the growth of the *Escherichia coli fabG* temperature-sensitive mutant CL104 under non-permissive conditions. *In vitro* assays demonstrated that FabG3 catalyses the reduction of 3-oxoacyl-acyl carrier protein (ACP) intermediates in fatty acid synthetic reactions, although FabG3 had a lower activity than FabG1. Moreover, the *fabG3* deletion did not affect growth or fatty acid composition. These results indicate that *Xcc fabG3* encodes a 3-oxoacyl-ACP reductase, but is not essential for growth or fatty acid synthesis. However, the *Xcc fabG3* knock-out mutant abolished xanthomonadin production, which could be only restored by wild-type *fabG3*, but not by other 3-oxoacyl-ACP reductase-encoding genes, indicating that *Xcc* FabG3 is specifically involved in xanthomonadin biosynthesis. Additionally, our study also shows that the *Xcc fabG3*-disrupted mutant affects *Xcc* virulence in host plants.

Keywords: 3-ketoacyl-acyl carrier protein reductase, xanthomonadin, *Xanthomonas campestris* pv. *campestris*.

INTRODUCTION

The *Xanthomonas* genus is a ubiquitous group of plant-associated bacterial pathogens that infect at least 124 monocotyledonous and 268 dicotyledonous plant species, many of which

are economically important crops or plants (Bonas *et al.*, 2000; Chan and Goodwin, 1999). A characteristic feature of the genus *Xanthomonas* is the production of yellow membrane-bound pigments called xanthomonadins, which are mixtures of water-insoluble, unusually brominated, aryl-polyene esters (Starr and Stephens, 1964). Xanthomonadins are useful chemotaxonomic and diagnostic indicators of *Xanthomonas* (Starr *et al.*, 1977). Moreover, xanthomonadins have roles in protecting against photobiological and peroxidative damage induced by host defence mechanisms and are required for epiphytic survival and host infection to maintain ecological fitness and virulence (Poplawsky *et al.*, 2000; Rajagopal *et al.*, 1997).

Xanthomonas campestris pv. *campestris* (*Xcc*) is the causal agent of black rot in crucifers (He and Zhang, 2008) and is also the producer of xanthan gum, a neutral and water-soluble polysaccharide that is widely used in a variety of products including medicine, foods and cosmetics. Thus, *Xcc* has great commercial and biotechnological application values (Kumar *et al.*, 2017). However, during the industrial production of xanthan gum, large amounts of ethanol are required to remove xanthomonadin impurities, so it is attractive to construct xanthomonadin-deficient strains by the deletion of genes in pigment synthesis (Dai *et al.*, 2018). In *Xcc*, the gene cluster for xanthomonadin biosynthesis (*pig*) contains seven transcriptional units, designated *pigA* to *G*, and consists of 22 open reading frames (ORF), encoding acyltransferase, ketoreductase, ketosynthase and dehydratase, which constitute part of a novel type II polyketide synthase pathway (He *et al.*, 2011; Poplawsky and Chun, 1997). *Xcc* utilizes 3-hydroxybenzoic acid (3-HBA), a diffusible factor with regulatory function, as the precursor for xanthomonadin synthesis, and 3-HBA is synthesized by a unique bifunctional chorismatase XanB2 (He *et al.*, 2011; Wang *et al.*, 2015; Zhou *et al.*, 2013a, b). Recently, Cao *et al.* (2018) reported only 11 genes are responsible for xanthomonadin biosynthesis, and *xanC* encodes an acyl carrier protein (ACP) while *xanA2*

*Correspondence: Email: wanghh36@scau.edu.cn

encodes the 3-HBA:ACP ligase to initiate xanthomonadin biosynthesis. However, further studies are required to define the detailed mechanisms of xanthomonadin synthesis.

Xcc uses quorum-sensing (QS) mechanisms mediated by molecules of the diffusible signal factor (DSF) family signals to regulate the expression of factors that contribute to virulence (He and Zhang, 2008; Zhou *et al.*, 2015). At least four DSF family signals have been identified in *Xcc*: DSF (*cis*-11-methyl-2-dodecenoic acid [11-Me-C₁₂: Δ^2]), BDSF (*cis*-2-dodecenoic acid [C₁₂: Δ^2]), CDSF (*cis*-11-methyldodeca-2,5-dienoic acid [11-Me-C₁₂: Δ^2 , Δ^5]) and IDSF (*cis*-10-methyl-2-dodecenoic acid [10-Me-C₁₂: Δ^2]) (Deng *et al.*, 2015, 2016; Zhou *et al.*, 2015). RpfF, with both acyl-ACP thioesterase and dehydratase activities, utilizes 3-hydroxyacyl-ACPs as substrates and is the key enzyme for DSF family signal biosynthesis. DSF family signals are involved in QS mechanisms that regulate pathogenicity by modulating the production of different virulence factors, such as extracellular enzymes, extracellular polysaccharides (EPS) and interspecies signalling, for example to influence the expression of a type III secretion system in *Pseudomonas aeruginosa* (Bi *et al.*, 2012; Zhou *et al.*, 2017).

Bacteria utilize a disassociated fatty acid synthase (FAS II) for *de novo* synthesis of fatty acids, which supply varieties of intermediates to other products, including lipids, vitamins (lipoic acid, biotin) and the 3-hydroxyacyl-ACPs for DSF family signals synthesis. The *Xcc* genome contains all of the genes required for FAS II, in which the key enzyme 3-oxoacyl-ACP reductase (OAR, FabG) is directly responsible for the synthesis of 3-hydroxyacyl-ACPs in the FAS II elongation cycle (Qian *et al.*, 2005; Yu *et al.*, 2016; Zhou *et al.*, 2015). Four genes, *fabG1* (XCC1018), *fabG2* (XCC0416), *fabG3* (XCC4003) and *fabG4* (XCC0384), encode putative OARs in the *Xcc* genome (Qian *et al.*, 2005). *fabG1* plays the major role in catalysing the reduction of 3-oxoacyl-ACPs in fatty acid synthesis. *fabG2* is a novel long-chain specific OAR that catalyses the reduction of long-chain ($\geq C_8$) 3-oxoacyl-ACPs but shows weak activity against shorter-chain (C₄, C₆) substrates (Hu *et al.*, 2018). The overexpression of *fabG1* or *fabG2* in *Xcc* led to a significant increase in the production of DSF family signals, while *fabG2* deletion resulted in reduced production of DSF family signals, which indicated that *Xcc* modulates the activity of OAR to control DSF family signal production (Hu *et al.*, 2018; Zhou *et al.*, 2015). In contrast, *fabG3* and *fabG4* appear to be involved in xanthomonadin and biotin synthesis, respectively, but their functions will necessitate experimental evidence.

In the present report, we characterized the functions of *fabG3* in the biosynthesis of xanthomonadins and DSF family signals using genetic complementation, biochemical analyses and gene deletion techniques. We found that *fabG3* possesses OAR activity *in vivo* and *in vitro*, but *fabG3* is not essential for growth or fatty acid synthesis. The *fabG3* deletion strain did not produce xanthomonadin, reduced the amounts of DSF family signals sharply and attenuated virulence to host plants.

RESULTS

Xcc fabG3 is not essential for growth, but is required for xanthomonadin biosynthesis

To identify the physiological functions of *fabG3* in cell growth and fatty acid synthesis, we attempted to disrupt *fabG3* with an in-frame deletion in the wild-type strain Xc1. First, the pK18mob-sacB-borne suicide plasmid pYYH-4 used to delete *fabG3* was constructed, and then it was introduced into the genome of *Xcc* wild-type strain by conjugal transfer from *Escherichia coli* S17-1. After negative selection mediated by *Bacillus subtilis* *sacB*, the *fabG3* deletion mutant strain YH1($\Delta fabG3$) was obtained and confirmed by colony PCR using the primers listed in Table S1 and by sequencing the allelic gene in the YH1 strain (Fig. S1). The expression of the neighbouring genes XCC4002 and XCC4004 was confirmed using RT-qPCR. The results showed expression of both genes was not affected in the mutant (Fig. S2A). Next, the growth of YH1 strain was tested in NYG medium. YH1 strain grew as well as the wild-type strain (Fig. S2B) under these conditions, suggesting that *fabG3* is not an essential gene for *Xcc*.

Xcc produces a mixture of organic solvent-extractable pigments, xanthomonadins, which are incorporated into the cell membrane, rendering the cells yellow in colour (Poplawsky and Chun, 1997). *Xcc fabG3* is located in the *pig* gene cluster, which is responsible for xanthomonadin synthesis. To determine whether *fabG3* functions in xanthomonadin synthesis, we compared the colony colour of mutant strain YH1 with wild-type strain on NYG plates. The colour of the wild-type was yellow, while the mutant strain YH1 appeared colourless on agar plates, indicating that *Xcc* YH1 strain did not produce xanthomonadins. However, the complemented strain *Xcc* YH2, which carried the wild-type *fabG3* in plasmid pYYH-5, turned yellow (Fig. 1A). The absorption spectra of the methanolic extracts were also recorded. Both the wild-type strain and *Xcc* YH2 showed peaks at 445 nm, while *Xcc* YH1 did not show a peak, confirming that *fabG3* mutant has little or no xanthomonadins (Fig. S3). The residual absorption seen at 445 nm for *Xcc* YH1 could be the result of the presence of intermediates in xanthomonadin synthesis (Rajagopal *et al.*, 1997).

Previously, xanthomonadins were shown to protect *Xanthomonas* from peroxidation damage and, if xanthomonadins are reduced, *Xanthomonas* is more sensitive to oxidative stress (Zhou *et al.*, 2013a). To assay oxidative stress resistance, hydrogen peroxide (H₂O₂) was added to cultures of *Xcc* YH1 strain at a final concentration of 880 μ M and the survival percentage after H₂O₂ treatment was determined. The wild-type strain maintained a c. 70% survival rate, while the *fabG3* deletion strain *Xcc* YH1 decreased the bacterial resistance to oxidative stress, as indicated by the 37% survival rate after H₂O₂ treatment. The expression of *fabG3* in *Xcc* YH1 restored H₂O₂ resistance to wild-type levels (Fig. 1B). Thus, *fabG3* is required for xanthomonadin synthesis, and the *fabG3* deletion resulted in *Xcc* being sensitive to H₂O₂.

We also supplemented 3-hydroxybenzoic acid (3-HBA), the precursor for xanthomonadin biosynthesis, and determined if it could restore *Xcc* YH1, as indicated by the colony turning yellow.

3-HBA failed to turn the *Xcc* YH1 colonies yellow, which suggested that the failure of *Xcc* YH1 was not due to a lack of precursor (Fig. 1A). Because *Xcc* XanB2 catalyses 3-HBA formation and plays a

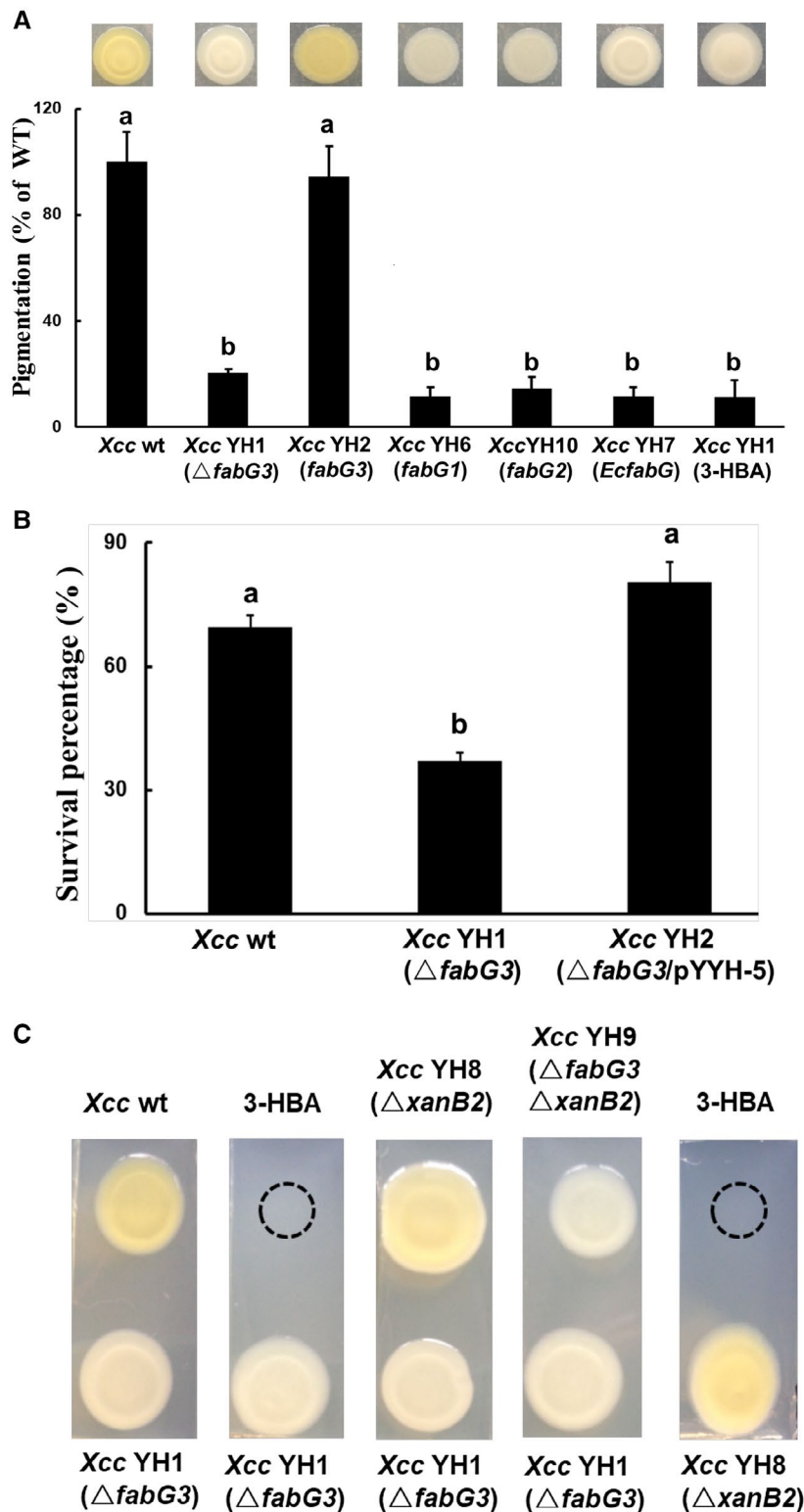


Fig. 1 The reduced xanthomonadin production and H₂O₂ resistance of the *Xcc* YH1 ($\Delta fabG3$) strain and restoration by *Xcc fabG3*. (A) Quantitative analysis of xanthomonadin production in *Xanthomonas campestris* pv. *campestris* (*Xcc*) strains. wt, wild-type; *fabG3*, complemented with plasmid pSRK-Km harbouring the gene *Xcc fabG3*; *Xcc fabG1*, complemented with plasmid pSRK-Km harbouring the gene *Xcc fabG1*; *Xcc fabG2*, complemented with plasmid pSRK-Km harbouring the gene *Xcc fabG2*; *EcfabG*, complemented with plasmid pSRK-Km harbouring the gene *Escherichia coli fabG*; 3-HBA, 3-hydroxybenzoic acid. (B) *Xcc* cells with an optical density of 1.0 when measured at 600 nm were collected for H₂O₂ treatment. After 30 min of H₂O₂ treatment, the CFU value of each strain was determined on NYG plates. Values shown are the means \pm standard deviations from three independent experiments. Different letters indicate significant difference between treatments based on the least significant difference at $P = 0.05$. (C) Diffusion plate assay showing the restoration of xanthomonadin production in $\Delta xanB2$ following exposure to *Xcc* YH1 ($\Delta fabG3$) or 3-HBA, and showing the failure to restore xanthomonadin production in *Xcc* YH1 ($\Delta fabG3$) following exposure to wide-type, $\Delta xanB2$ or 3-HBA.

vital role in xanthomonadin biosynthesis (He *et al.*, 2011), we further constructed the *xanB2* deletion strain *Xcc* YH8 and the *xanB2fabG3* double-deletion strain *Xcc* YH9 using the homologous recombination method. As previously reported, *Xcc* YH8 ($\Delta xanB2$) failed to produce xanthomonadin and colonies were colourless on agar plates, but addition of 3-HBA in the vicinity of the colony turned *Xcc* YH8 colonies yellow (He *et al.*, 2011). *Xcc* YH8 ($\Delta xanB2$) also restored xanthomonadin production when exposed to *Xcc* YH1. However, *Xcc* YH9 ($\Delta xanB2\Delta fabG3$) could not be restored to the wild-type phenotype by exposure to the *Xcc* YH1 strain (Fig. 1C). The diffusion plate assay also showed that *Xcc* YH1 did not turn yellow when grown in the vicinity of wild-type or *Xcc* YH8 ($\Delta xanB2$) (Fig. 1C). Thus, *Xcc* YH1 produced 3-HBA, and *Xcc* FabG3 was involved downstream of 3-HBA in xanthomonadin biosynthesis.

***Xcc fabG3* complemented the growth of the *E. coli fabG* temperature-sensitive mutant under non-permissive temperature**

Although *Xcc fabG3* is located in the *pig* gene cluster and involved in xanthomonadin synthesis, protein sequence alignments showed that *Xcc* FabG3 is 42% identical with *E. coli* FabG (Lai and Cronan,

2004), and 40% identical with *Xcc* FabG1 (Fig. 2). *Xcc* FabG3 contains the short-chain dehydrogenase/reductase (SDR) family's catalytically active triad (Ser, Tyr and Lys) and the N-terminal cofactor-binding sequence (Gly motif [GlyXXGlyXXGly]) defined by the X-ray crystal structure of *E. coli* FabG (Mao *et al.*, 2016). Two *E. coli* FabG residues, Arg-129 and Arg-172, which play critical roles in facilitating the binding of the ACP moiety of the substrate, were also conserved in *Xcc* FabG3 (Feng *et al.*, 2015) (Fig. 2). Thus, we hypothesized that *Xcc fabG3* encodes a functional OAR. To test this hypothesis, *Xcc fabG3* was inserted into the arabinose-inducible vector pBAD24M to produce the expression construct pYYH-2, which was further transferred into the *E. coli fabG* temperature-sensitive strain CL104 (Lai and Cronan, 2004). The resulting transformant was tested for growth at a non-permissive temperature (42 °C). The strain CL104 carrying pYYH-2 grew well at 42 °C on rich broth (RB) plates in the presence of arabinose (Fig. 3A). However, in RB liquid medium with an arabinose inducer, the CL104 strain carrying pYYH-2 showed a reduced growth rate compared with that of CL104 carrying *Xcc fabG1* or *E. coli fabG* (Fig. 3B). These results preliminarily indicated that *Xcc fabG3* could complement the *E. coli fabG* (ts) strain CL104, but *Xcc* FabG3 appeared to be less active than *Xcc* FabG1 or *E. coli* FabG.

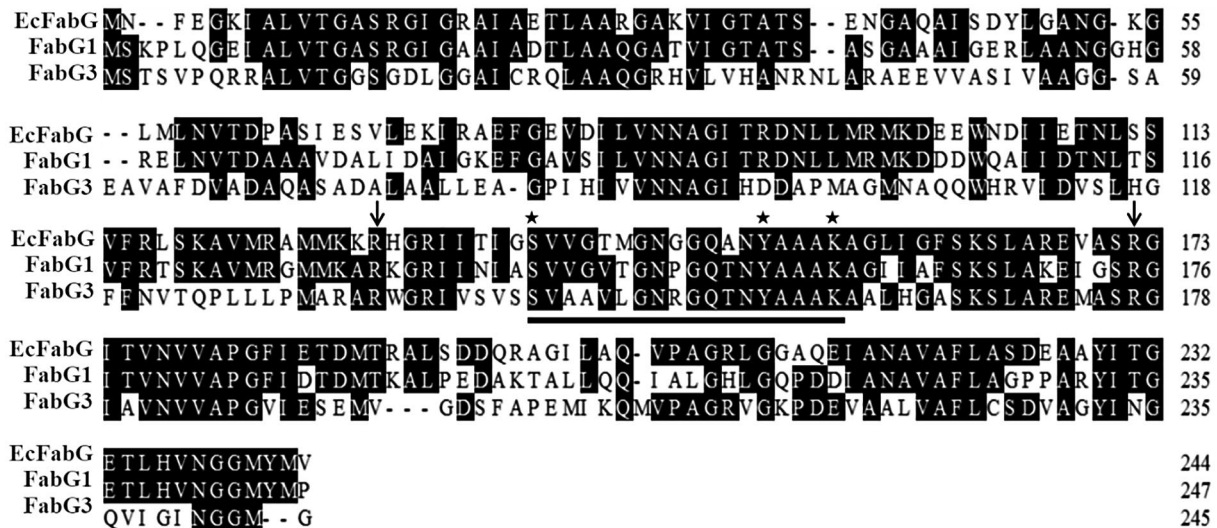


Fig. 2 Alignment of *Xanthomonas campestris* pv. *campestris* (*Xcc*) FabG3 with *Escherichia coli* FabG (EcFabG) and *Xcc* FabG1. The two arginine residues thought to bind the acyl carrier protein (ACP) moiety are indicated by arrows and the catalytic triad residues are indicated by asterisks. The alignment was performed with ClustalW based on identical residues.

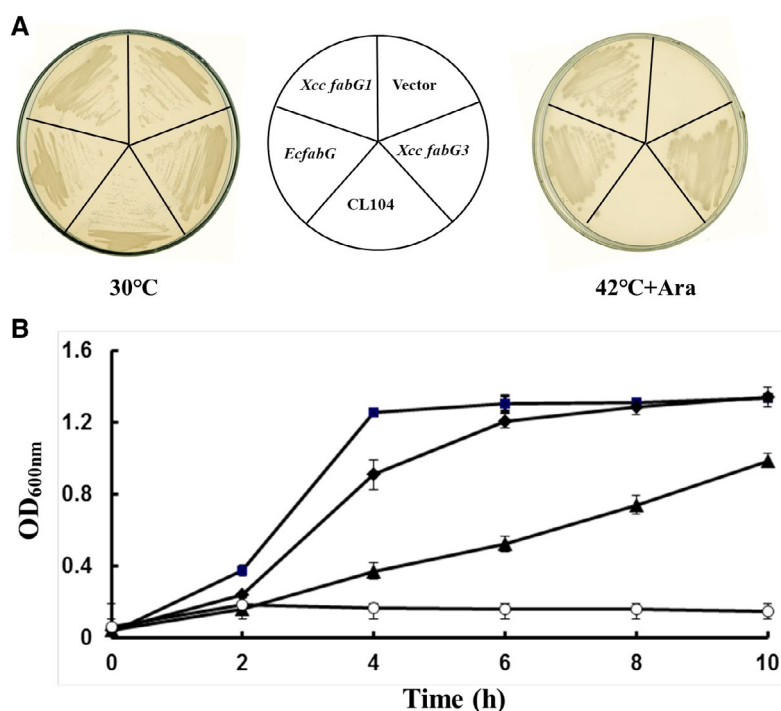


Fig. 3 Growth of *Escherichia coli fabG* (ts) mutant CL104 transformants containing plasmids carrying *Xanthomonas campestris* pv. *campestris* (*Xcc fabG3*, *Xcc fabG1* and *E. coli fabG*). (A) *E. coli* CL104 derivatives, carrying the pBAD24M-derived plasmids pHWG (pBAD-*EcfabG*), pYYH-1 (pBAD-*Xcc fabG1*) and pYYH-2 (pBAD-*Xcc fabG3*), were grown at 30 °C or 42 °C on LB plates in the presence of 0.01% arabinose. (B) Transformants of *E. coli fabG* (ts) mutant CL104 with pBAD24M-derived plasmids grown in LB liquid containing 0.01% arabinose. Squares, CL104/pHWG (pBAD-*EcfabG*); diamonds, CL104/pYYH-1 (pBAD-*XccfabG1*); triangles, CL104/pYYH-2 (pBAD-*Xcc fabG3*); empty circles, CL104/pBAD24M. Data are means \pm standard deviations of three independent assays.

Xcc FabG3 possesses OAR activity *in vitro*

To determine whether *Xcc FabG3* possesses OAR activity *in vitro*, the N-terminal 6 \times His-tagged *Xcc FabG3* recombinant protein was expressed in *E. coli* BL21 (DE3) and purified by nickel chelate chromatography (data not shown). Other bacterial fatty acid biosynthetic proteins were also purified as described in the 'Experimental procedures' section.

First, the initiation step of the fatty acid synthesis reaction was reconstituted. *Escherichia coli* FabD, FabH, FabZ, FabI and OAR (*E. coli* FabG or *Xcc FabG3*) were added sequentially. After incubation for 1 h, the reaction mixture was analysed by conformationally sensitive gel electrophoresis. In the absence of OAR, only holo-ACP was seen (Fig. 4A, Lane 4). The addition of *Xcc FabG3* to the reaction mixture, like the reaction mixture containing *E. coli* FabG, resulted in the production of butyryl-ACP (Mao *et al.*, 2016) (Fig. 4A, lanes 2 and 3). Next, the enzymatic activity of *Xcc FabG3* in the reduction of long-chain 3-ketoacyl-ACP substrates was also determined. These reactions were reconstituted by adding malonyl-ACP, octanoyl-ACP, *Ralstonia solanacearum* RSp0194, OAR (*E. coli* FabG or *Xcc FabG3*), *E. coli* FabZ and FabI, and co-factors NADPH and NADH. In these reactions *R. solanacearum* RSp0194 condensed octanoyl-ACP with malonyl-ACP to produce 3-oxodecanoyl-ACP. Then, if *Xcc FabG3* possessed OAR activity,

3-oxodecanoyl-ACP was reduced to 3-hydroxydecanoyl-ACP. After dehydration catalysed by *E. coli* FabZ and reduction by FabI, 3-hydroxydecanoyl-ACP was converted to decanoyl-ACP. Both reaction mixtures, containing either *E. coli* FabG or *Xcc FabG3*, formed decanoyl-ACP (Fig. 4B, lanes 2 and 3). These data further confirmed that, like *E. coli* FabG, *Xcc FabG3* could reduce 3-oxoacyl-ACP to 3-hydroxyacyl-ACP *in vitro* and that *Xcc fabG3* encoded a functional OAR.

The OAR activities of *Xcc FabG3* were also assayed using various chains of 3-oxoacyl-ACPs as substrates, by monitoring the decrease in NADPH absorbance at 340 nm. *Xcc FabG3* exhibited reductive activities with wide range of substrate specificities, from 3-oxobutyryl ACP (C_4) to 3-oxododecanoyl ACP (C_{12}). However, the reductive activity of *Xcc FabG3* was much less than that of *Xcc FabG1*, from c. 10% for 3-oxododecanoyl ACP (C_{12}) to c. 50% for 3-oxodecanoyl ACP (C_{10}) (Table 1). These data explain why the *E. coli* CL104 strain carrying pYYH-1 (with *Xcc fabG3*) grew much more slowly than the CL104 strain carrying pYYH-1 (with *Xcc fabG1*) (Fig. 3B). We also compared the abilities of *Xcc FabG1* and *Xcc FabG3* to reduce the model substrate acetoacetyl-CoA. *Xcc FabG3* failed to reduce acetoacetyl-CoA, while *Xcc FabG1* reduced acetoacetyl-CoA with a maximal rate of 610.0 ± 58.0 $\mu\text{mol}/\text{min}$.

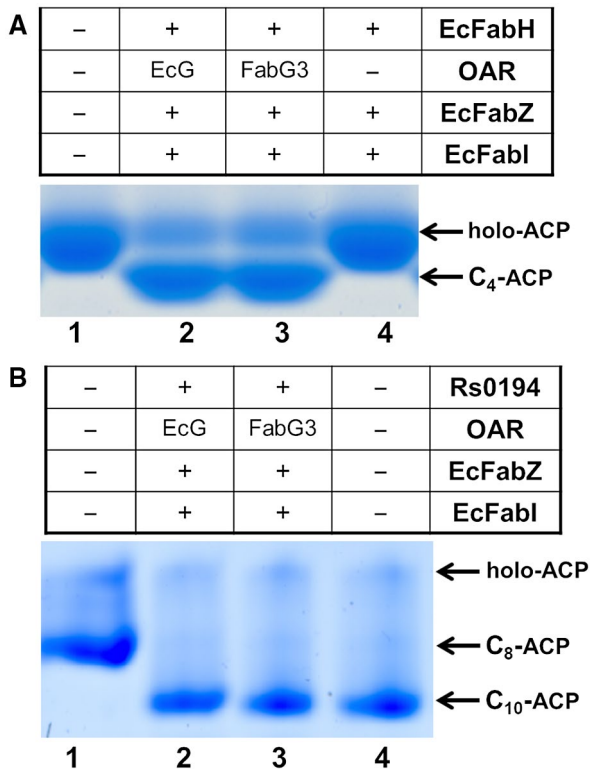


Fig. 4 Assay of the *in vitro* fatty acid synthesis abilities of *Xanthomonas campestris* pv. *campestris* (*Xcc*) FabG3. (A) Function of *Xcc* FabG3 in the initial cycle of fatty acid synthesis. Lane 1, holo-ACP; lane 2, reaction product containing *E. coli* FabG; lane 3, reaction product containing *Xcc* FabG3; lane 4, reaction product without 3-ketoacyl-ACP reductase. (B) Functions of *Xcc* XabG in the elongation cycle of fatty acid synthesis. Lane 1, product of octanoyl-ACP synthesized by *Vibrio harveyi* AasS; lane 2, reaction product catalysed by *E. coli* FabG; lane 3, reaction product catalysed by *Xcc* FabG3; lane 4, product of decanoyl-ACP synthesized by *V. harveyi* AasS. EcG, *E. coli* FabG; OAR, 3-oxoacyl-ACP reductase; EcFabH, *E. coli* 3-ketoacyl-ACP synthase III; EcFabZ, *E. coli* 3-hydroxyacyl-ACP dehydrase; EcFabI, *E. coli* enoyl-ACP reductase.

Xcc FabG3 is specific for xanthomonadin biosynthesis

A deletion of *fabG3* caused *Xcc* to abolish the production of xanthomonadins. *Xcc* FabG3 possessed OAR activity, even though this activity was much lower than that of *Xcc* FabG1. Thus, we hypothesized that other OAR-encoding genes might restore the *fabG3* deletion mutant strain to produce xanthomonadins. To confirm this hypothesis, *Xcc fabG1*, *Xcc fabG2* and *E. coli fabG*-encoding plasmids were independently introduced into YH1 ($\Delta fabG3$) strain, and the production of xanthomonadins was determined. Unfortunately, the OAR-encoding genes did not restore xanthomonadin production in YH1 ($\Delta fabG3$), suggesting that *Xcc* FabG3 plays a unique role in xanthomonadin biosynthesis and that other OAR enzymes might not functionally replace *Xcc* FabG3 in xanthomonadin biosynthesis (Fig. 1A). For further confirmation, the fatty acid composition of strain *Xcc* YH1 grown in NYG medium was determined by gas chromatography-mass

Table 1 *Xanthomonas campestris* pv. *campestris* (*Xcc*) FabG1 and *Xcc* FabG3 activities with various 3-oxoacyl-ACPs*

Substrate	<i>Xcc</i> FabG1 (μ moles/mg/min)	<i>Xcc</i> FabG3 (μ moles/mg/min)
3-oxobutyryl ACP	14.69 \pm 0.75 c	4.65 \pm 0.44 c
3-oxohexanoyl ACP	24.15 \pm 2.06 a	8.10 \pm 0.89 a
3-oxooctanoyl ACP	22.31 \pm 1.91 a	7.76 \pm 0.97 b
3-oxodecanoyl ACP	17.94 \pm 1.68 b	8.53 \pm 1.06 a
3-oxododecanoyl ACP	17.21 \pm 2.10 b	1.74 \pm 0.11 d

*The values are the means \pm standard deviations of three independent experiments. The statistical analyses were performed in Microsoft Excel with *P* values between each pairwise comparison calculated by two-tailed Student's *t*-tests. Significant differences are indicated by different letters (*P* < 0.05).

spectrometry (GC-MS) (Table S2). The fatty acid composition of *Xcc* YH1 was similar to that of wild-type strain, which suggested that *Xcc* FabG3 might not be involved in fatty acid synthesis and provided evidence to support *Xcc* FabG3 being specific for xanthomonadin biosynthesis.

Xcc fabG3 deletion mutant has attenuated virulence

To investigate the role of *fabG3* in the virulence regulation of *Xcc*, the pathogenesis of *fabG3* deletion mutant *Xcc* YH1 was determined on plants. A leaf clipping virulence assay using Chinese radish was conducted (Dow *et al.*, 2003). The average lesion length caused by the wild-type strain on a leaf of Chinese radish was 17.6 mm 2 weeks after inoculation (Fig. 5). The *Xcc fabG3* deletion strain resulted in a significantly reduced average lesion length (9.5 mm), while the average lesion length of the *fabG3*-complemented strain (14.7 mm) was not significantly different from that of the wild-type (Fig. 5). We also determined the growth of *Xcc* strains in fully mature Chinese cabbage (Wongbok) extracts, and the *fabG3* deletion mutant grew as well as the wild-type (data not shown). These data showed that *Xcc fabG3* contributed to virulence.

We also evaluated several pathogenicity-related virulence factors produced by *Xcc* strains. The activities of extracellular enzymes, including cellulase, amylase and protease, were first tested. The production of the three extracellular enzymes was not statistically different between the *fabG3* deletion mutant and the wild-type (Fig. S4A). Next, extracellular polysaccharide (EPS) production by *Xcc* strains was determined. The amounts of EPS produced in wild-type, *Xcc* YH1 ($\Delta fabG3$) and complemented strain *Xcc* YH2 were not statistically different.

Xcc FabG3 is involved in DSF biosynthesis

Thus far we have shown that FabG3 is an OAR and the deletion of *fabG3* causes *Xcc* to have a reduced virulence on host plants. To determine whether *Xcc fabG3* affected the synthesis of DSF

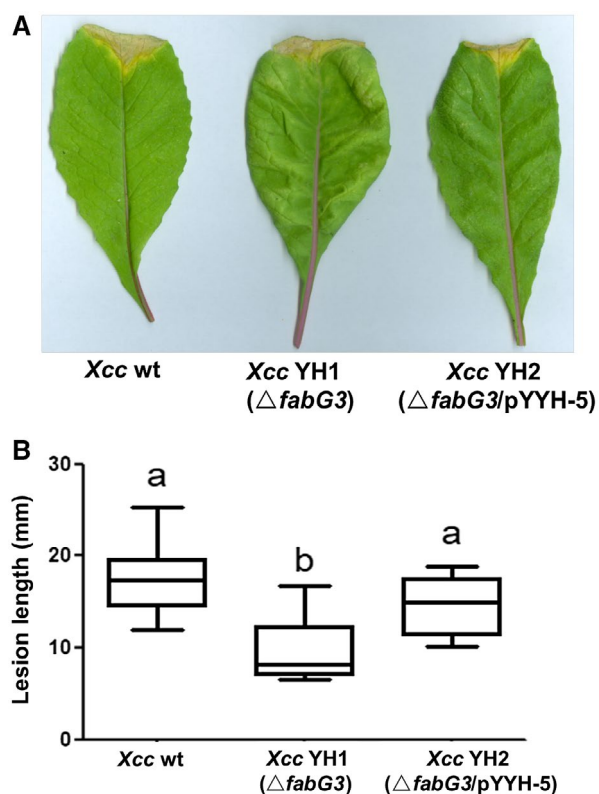


Fig. 5 The effects of the *Xanthomonas campestris* pv. *campestris* (*Xcc*) *fabG3* deletion on the virulence of *Xcc*. (A) Pathogenicity test on Chinese radish with the *Xcc* wild-type (wt) strain, *Xcc fabG3*-deletion mutant strain *Xcc* YH1 and complementary strain *Xcc* YH2. (B) Test of the virulence of the *Xcc* strains by measuring lesion length after introducing bacteria into the vascular system of Chinese radish by leaf clipping. Values are expressed as the means and standard deviations of triplicate measurements, each comprising ten leaves. Different letters indicate significant differences between treatments ($P = 0.05$).

family signals, we analysed their production in the *fabG3* deletion mutant strain. We tested the production of DSF family signals in *Xcc* YH1 using a bioassay in which *Xcc* FE58 (Wang *et al.*, 2004) was the reporter strain. The blue halo that formed around *Xcc* YH1 was smaller than that around the wild-type strain, indicating that YH1 decreased the production of DSF family signals (Fig. 6A). Furthermore, we extracted and purified the DSF family signals from the supernatants, and analysed them quantitatively using liquid chromatography-mass spectrometry (LC-MS). The results proved that BDSF and DSF production in the *fabG3* mutant *Xcc* YH1 decreased to 46.9% and 35.3%, respectively, and the complemented strain *Xcc* YH2 recovered the DSF family signals production to the wild-type level (Fig. 6B).

Because *rpfC*-deletion strain XC1 ($\Delta rpfC$) produced greater concentrations of DSF family signals (He *et al.*, 2006), we further deleted *fabG3* in XC1 ($\Delta rpfC$), producing *rpfC* and *fabG3* double deletion mutant *Xcc* YH3. The complemented strain *Xcc* YH4

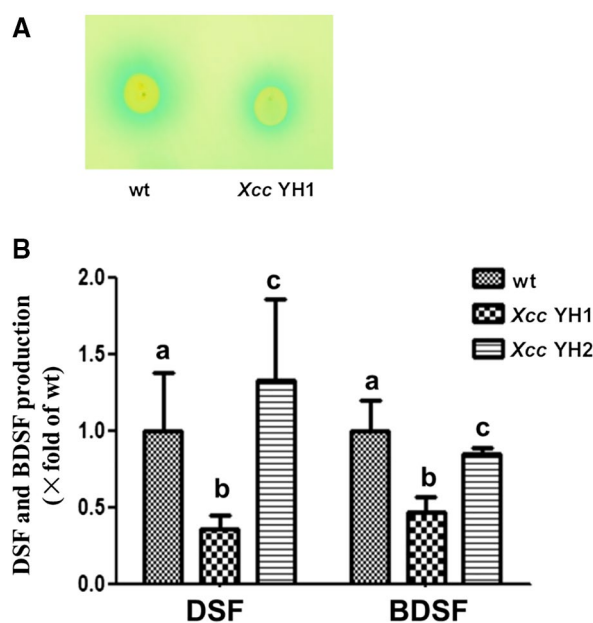


Fig. 6 The effects of *Xanthomonas campestris* pv. *campestris* (*Xcc*) *fabG3* deletion on the production of DSF family signals. (A) DSF family signal bioassay of *Xcc* strains. The formation of a blue halo owing to hydrolysis of 5-bromo-4-chloro-3-indolyl- β -D-glucuronic acid around the site of inoculation indicates the presence of DSF-like activity. (B) DSF family signals produced by *Xcc fabG3* deletion and complemented strains. Supernatants of 20 mL of *Xcc* strains grown in NA medium for 24 h were collected, and DSF family signals were detected with the liquid chromatography-mass spectrometry (LC-MS) method. In strain *Xcc* YH1 the *Xcc fabG3* gene was deleted in the wild-type strain; strain *Xcc* YH2 has *Xcc fabG3* being complemented by the plasmid pSRK-Km in *Xcc* YH2. The relative amounts of signal molecules were calculated on the basis of their peak areas. The data shown are the means of the results of three repeats and error bars indicate standard deviations. Different letters indicate significant differences between treatments based on the least significant difference at $P = 0.05$.

harbouring plasmid pYYH-5 (carrying *fabG3*) was also obtained. The DSF family signals in these *Xcc* strains were extracted and separated using high-performance liquid chromatography (HPLC) (Fig. S5A). After incubation in NA medium for 24 h, DSF, BDSF and IDSF signal productions in *Xcc* YH3 ($\Delta fabG3$) decreased sharply to 36.5%, 19.0% and 12.5%, respectively, compared with those produced by the parent strain $\Delta rpfC$. The complemented strain even produced greater amounts of DSF family signals compared with those observed in $\Delta rpfC$ (Fig. S5B). Thus, *Xcc* FabG3 contributed to DSF family signals production. Moreover, to investigate whether expression of *Xcc fabG3* in the parent strain $\Delta rpfC$ increased the production of DSF family signals, we introduced *fabG3*-encoding plasmid pYYH-5 into $\Delta rpfC$ strain and the production of DSF family signals was determined. The results confirmed that *fabG3* overexpression led to the significantly increased production of DSF family signals in $\Delta rpfC$ (Fig. S5B). Because FabG3 showed OAR activity, this finding was consistent with previous studies in which the overexpression of two other OAR-encoding genes (*fabG1* and

fabG2) in *Xcc* led to a significant increase in DSF family signals production (Hu *et al.*, 2018; Zhou *et al.*, 2015). Thus, it may be that the OAR activity in *Xcc* cells, rather than the presence of *fabG3*, is important for DSF family signals synthesis. We further examined the OAR activity in cell-free extracts of *Xcc* strains using 3-oxoacyl-ACP as a substrate and confirmed the above conclusion. The activity of *Xcc*YH3 ($\Delta fabG3$) ($0.07 \pm 0.02 \mu\text{mol/mg per min}$) was only half the total OAR activity of $\Delta rpfC$ strain ($0.15 \pm 0.04 \mu\text{mol/mg per min}$). The OAR activity in the complemented strain *Xcc* YH4 and the *fabG3* overexpression strain *Xcc* YH5 increased to $0.21 \pm 0.07 \mu\text{mol/mg per min}$ and $0.30 \pm 0.06 \mu\text{mol/mg per min}$, respectively (Fig. S5C). These results confirmed that *Xcc* modulated the total OAR activity in cells to control the production of DSF family signals.

DISCUSSION

OAR catalyses the first reduction of 3-oxoacyl-ACP to 3-hydroxyacyl-ACP in the type II fatty acid synthase systems of bacteria (Magnuson *et al.*, 1993). Although *fabG* is the only gene that encodes OAR activity in *E. coli*, multiple *fabG* paralogues have been reported in other species, and some are involved in fatty acid biosynthesis under special conditions (Feng *et al.*, 2015; Mao *et al.*, 2016). The *Xcc* genome encodes several FabG paralogues (Qian *et al.*, 2005): FabG1 is the housekeeping OAR, while FabG2 is a novel OAR specific to reduce long-chain 3-oxoacyl-ACP substrates (Hu *et al.*, 2018). In this report, we confirmed that *Xcc fabG3* encodes an OAR enzyme. First, *fabG3* improved the growth of *E. coli fabG(ts)* strain CL104. Second, *Xcc FabG3* catalysed the reduction of 3-oxoacyl-ACPs with varied chain lengths in the elongation cycle of FAS II *in vitro*. However, *Xcc FabG3* seems distinct from *Xcc FabG1*. *Xcc fabG1* is essential for growth and fatty acid synthesis, and cannot be deleted from the chromosome. However, *Xcc fabG3* is not essential, and the *fabG3* deletion strain was viable, producing similar species and amounts of fatty acids as the wild-type strain. Additionally, the OAR activity of *Xcc FabG3* was much lower than that of *Xcc FabG*, only ranging from 10% to 50% depending on the substrates. Moreover, *Xcc FabG3* shows no reductive activity on the model substrate acetoacetyl-CoA, but *Xcc FabG1* possesses a high reductive ability.

The membrane-bound yellow pigment xanthomonadins play essential roles in protecting bacteria from photobiological and peroxidative damage (Poplawsky and Chun, 1998; Rajagopal *et al.*, 1997), but xanthomonadin biosynthesis mechanism needs further study. In our study, *Xcc fabG3* deletion abolished xanthomonadin production, which indicated that FabG3 plays a vital role in xanthomonadin synthesis. Cao *et al.* (2018) identified 11 genes (named *xanA2* to *xanM*, respectively) within the *pig* cluster as being essential for xanthomonadin synthesis, in which the ketoreductase-coding gene *xanH* corresponds to *fabG3* in this study.

3-HBA, the precursor for xanthomonadin biosynthesis (Zhou *et al.*, 2013b), could not restore the xanthomonadin production in the *Xcc fabG3* mutant, implying that FabG3 catalyses the reduction of the 3-keto group of an unknown intermediate downstream in the xanthomonadin synthetic pathway. At present, three OAR-coding genes, *fabG1*, *fabG2* and *fabG3*, have been identified in the *Xcc* genome; only *fabG3* expression in the mutant could restore xanthomonadin production, but *Xcc fabG1*, *fabG2* and *E. coli fabG* could not independently complement the xanthomonadin-deficient phenotype. The results indicate that FabG3 plays a unique role in the xanthomonadin synthetic pathway, and its function cannot be replaced by other OARs. Our data revealed that the reductase activity of FabG1 is much greater than that of FabG3. Moreover, *fabG1* is comparatively highly expressed and is a housekeeping gene that cannot be deleted directly. The white colony appearance of the *fabG3* deletion mutant also demonstrated that FabG1 in the cell cannot functionally replace FabG3 in xanthomonadin synthesis. Based on the gene cluster, xanthomonadin is synthesized by a novel type II polyketide synthase pathway (He *et al.*, 2011), and we propose a model reductive reaction catalysed by *Xcc FabG3* in Fig. 7. However, the substrate(s) and catalytic mechanism of *Xcc FabG3* need further study.

Xcc RpfF, the key enzyme for the biosynthesis of the DSF family signals, utilizes 3-hydroxyacyl-ACPs as substrates (Zhou *et al.*, 2015), while 3-hydroxyacyl-ACPs are the products of OAR in the bacterial fatty acid synthetic pathway (Rafferty *et al.*, 1998). Thus, the production of DSF family signals is closely associated with OAR activity. In this report, we found *Xcc FabG3* had OAR activity *in vivo* and *in vitro*, and it is reasonable that *Xcc fabG3* null mutant decreased DSF family signals production, while a wild-type *fabG3*-encoding plasmid restored the high production level of DSF family signals. These results are consistent with our previous research. Hu *et al.* (2018) reported that *Xcc fabG2* deletion mutant produced <50% of DSF family signals of wild-type, and overexpression of *fabG1* or *fabG2* resulted DSF family signals levels 50% greater than wild-type. Therefore, we concluded that *Xcc* might modulate the total OAR activity to control the production of DSF family signals.

In the study, *Xcc fabG3* deletion resulted in a substantial reduction in virulence, which was restored to wild-type level by complementation with plasmid expressing *fabG3*. During the system infection process, *Xcc* produces a variety of pathogenic factors, including EPS and extracellular enzymes (cellulose, amylase and protease), under the regulation of a DSF-mediated QS system. However, the pathogenic factor productions were not statistically different between the *fabG3* deletion mutant and wild-type strain, indicating that the pathogenic factors' reduction was not the cause for virulence attenuation. Because xanthomonadins protect *Xcc* from photooxidative damage, abolishment of xanthomonadins in the *fabG3* deletion mutant is the most probable reason for virulence reduction. Moreover, the survival rate of *fabG3* deletion mutant was much lower than that of wild-type when exposed

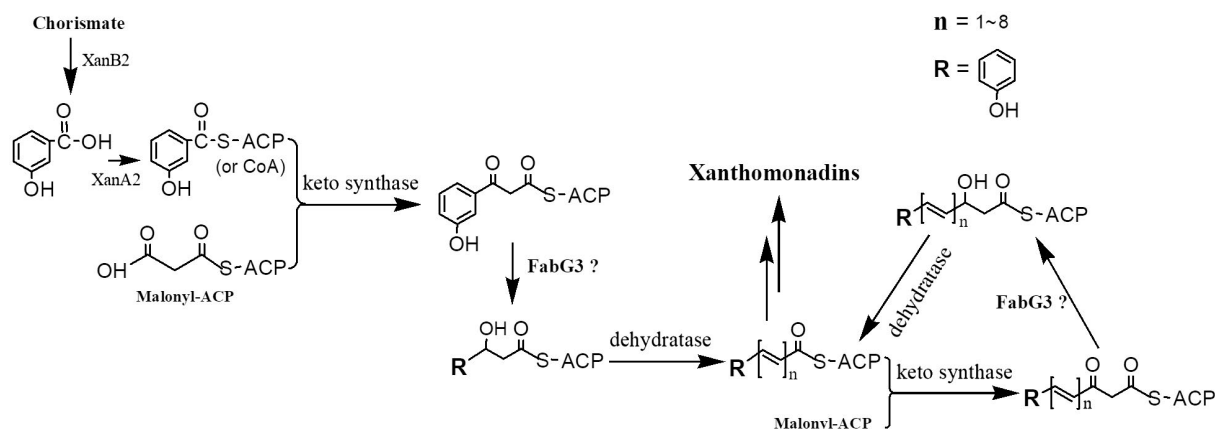


Fig. 7 The proposed biosynthetic pathway for xanthomonadins in *Xanthomonas campestris* pv. *campestris*. The precursor 3-hydroxybenzoic acid is ligated to ACP (or CoA) by XanA2. *Xcc3998* and *Xcc4004* in the *pig* cluster are proposed to encode the keto synthase and dehydratase, respectively, involved in xanthomonadin biosynthesis.

to oxidative stress (H_2O_2), which is a common environmental cue that pathogens encounter during systemic invasion. Similar findings were reported by Poplawsky and Chun (1998). When *xanB2*, an essential gene for xanthomonadins synthesis, was disrupted, the mutant virulence reduced sharply (He *et al.*, 2011).

EXPERIMENTAL PROCEDURES

Materials

Malonyl-CoA, acetyl-CoA, acetoacetyl-CoA, fatty acids, NADH, NADPH and antibiotics were purchased from Sigma (USA). Takara Biotechnology Co. (Japan) provided molecular biology reagents. Novagen (USA) provided pET vectors. Invitrogen (USA) provided Ni-agarose columns. GE Healthcare (USA) provided the HiTrap Q strong anion-exchange column and Bio-Rad (USA) provided the Quick Start Bradford dye reagent. All other reagents were of the highest available quality. Oligonucleotide primers were synthesized by TaKaRa Biotechnology Co.

Bacterial strains, plasmids and growth conditions

The strains and plasmids are listed in Table 2. *Escherichia coli* strains were grown in Luria-Bertani (LB) medium at 37 °C. The phenotypes of *E. coli fab* strains were assessed on RB medium (Ulrich *et al.*, 1983). The *Xcc* strains were grown at 30 °C in NYG medium (tryptone 5 g/L, yeast extract 3 g/L, glycerol 20 g/L) (Yu *et al.*, 2016). When required, antibiotics and inducers were added as follows: sodium ampicillin 100 µg/mL, kanamycin sulphate 30 µg/mL, gentamycin 30 µg/mL for *E. coli* or 10 µg/mL for *Xcc*, rifampicin 50 µg/mL, arabinose 100 µg/mL, isopropyl-β-D-thiogalactoside (IPTG) 240 µg/mL. Bacterial growth was determined by growing on solid media or by measuring the optical density at 600 nm.

Plasmids construction

Xcc fabG3 was amplified from genomic DNA of wild-type strain *Xcc8004* with primers *fabG3* P1 (*Nde*I) and *fabG3* P1 (*Hind*III) listed in Table S1. The PCR was performed with *Pfu* DNA polymerase and the product was inserted into the pMD19-T vector to obtain plasmid pYYH-1. The *Xcc fabG3* gene was confirmed by sequencing performed by Shanghai Sangon, Inc. (Shanghai, China). The *Xcc fabG3* gene was digested with *Nde*I and *Hind*III, isolated and ligated into pBAD24M (Cheng *et al.*, 2012) to create plasmid pYYH-2. The *fabG3* gene was also inserted into pET-28b to produce pYYH-3, and into pSRK-Km (Khan *et al.*, 2008) to produce pYYH-5. The *Xcc fabG1* gene was amplified and cloned into pSRK-Km to create pYYH-6 and into pBAD24M to create plasmid pYYH-8.

Disruption of *Xcc fabG3* or *Xcc xanB2* in the chromosome

To disrupt the *Xcc fabG3* gene, upstream (with an *Eco*RI site at the end) and downstream (with a *Hind*III site at the end) fragments of *Xcc fabG3* (called *fabG3* Up and *fabG3* Dn, respectively) were amplified from *Xcc* genomic DNA with *Pfu* DNA polymerase, using the primer pairs *fabG3* Up1/Up2 for *fabG3* Up and *fabG3* Down3/Down4 for *fabG3* Dn (Table S1). The PCR products were purified and an overlap extension was carried out using *fabG3* Up1 and *fabG3* Down4 as primers. The fused fragment was then digested with *Eco*RI and *Hind*III and inserted into plasmid pK18mobsacB (Schafer *et al.*, 1994) cut with the same enzymes to produce the suicide plasmid pYYH-4.

Following the mating of derivatives of *E. coli* S17-1 carrying pYYH-4 with *Xcc* on NYG plates for 36 h at 30 °C, the cells were suspended in NYG medium and appropriate dilutions were spread onto NYG plates containing rifampicin plus kanamycin (resistant form of the plasmid pYYH-4) to select for the single-crossover integrants. Several single-crossover integrant colonies were

Table 2 Bacterial strains and plasmids used in this study

Bacterial strain	Relevant characteristics*	Source
<i>Escherichia coli</i>		
DH-5 α	F ⁻ <i>deoR endA1 gyrA96 hsdR17(r_K⁻m_K⁺) recA1 relA1 supE44 thi-1 Δ(<i>lacZYA-argF</i>)U169(ϕ80/<i>lacZ</i>ΔM15)</i>	Laboratory stock
BL21(DE3)	F ⁻ <i>dcm ompT hsdS</i> (r _B ⁻ m _B ⁻) <i>gal</i> (λ DE3)	Laboratory stock
S17-1	Tp ^r Sm ^r <i>recA thi pro hsdR</i> (RP4-2 Tc::Mu Km::Tn7), λ <i>pir</i>	Laboratory stock
CL104	<i>fabG</i> (ts) <i>panD</i> Cm ^r , Tet ^r , Km ^r	Laboratory stock
MG1655	Wild-type	Laboratory stock
<i>Xanthomonas campestris</i> pv. <i>campestris</i>		
XC1	Rif ^r , wild-type	Qian <i>et al.</i> (2005)
FE58	Rif ^r , Tc ^r , <i>rpfF</i> ::Tn5 <i>lac</i> , Biosensor for DSF signals	Wang <i>et al.</i> (2004)
YH1	Rif ^r , Δ <i>fabG3</i>	This study
YH2	Rif ^r , Km ^r , <i>Xcc</i> YH1/pYYH-5	This study
XC1(Δ <i>rpfC</i>)	Rif ^r , XC1 Δ <i>rpfC</i>	Zhou <i>et al.</i> (2015)
YH3	Rif ^r , XC1 Δ <i>rpfC</i> Δ <i>fabG3</i>	This study
YH4	Rif ^r , Km ^r , <i>Xcc</i> YH3/pYYH-5	This study
YH5	Rif ^r , Km ^r , XC1 Δ <i>rpfC</i> /pYYH-5	This study
YH6	Rif ^r , Km ^r , <i>Xcc</i> YH1/pYYH-6	This study
YH7	Rif ^r , Km ^r , <i>Xcc</i> YH1/pYYH-7	This study
YH8	Rif ^r , <i>Xcc</i> 8004 Δ <i>XanB2</i>	This study
YH9	Rif ^r , <i>Xcc</i> 8004 Δ <i>XanB2</i> Δ <i>fabG3</i>	This study
YH10	Rif ^r , Km ^r , <i>Xcc</i> YH1/pYYH-10	This study
Plasmids		
pET-28b	Km ^r , T7 promoter-based expression vector	Novagen
pMD19-T	Amp ^r , TA cloning vector	Takara
pSRK-Km	Km ^r , broad-host-range expression vector containing <i>lac</i> promoter and <i>lacI</i> , <i>lacZ</i> α ⁺	Khan <i>et al.</i> (2008)
pK18mobscaB	Km ^r , <i>sacB</i> -based gene replacement vector	Schafer <i>et al.</i> (1994)
pBAD24M	Amp ^r ; pBAD24 <i>NcoI</i> site replaced by <i>NdeI</i> site	Zhu <i>et al.</i> (2013)
pHWG	Amp ^r , <i>EcfabG</i> gene cloned into plasmid pBAD24M	Lab stock
pYYH-1	Amp ^r , <i>Xcc fabG3</i> gene cloned into plasmid pMD19-T	This study
pYYH-2	Amp ^r , <i>Xcc fabG3</i> gene cloned into plasmid pBAD24M	This study
pYYH-3	Km ^r , <i>Xcc fabG3</i> cloned into plasmid pET-28b	This study
pYYH-4	Km ^r , about 1000 bp <i>Xcc fabG3</i> deletion DNA fragment inserted into pK18mobscaB between <i>EcoRI</i> / <i>HindIII</i> sites	This study
pYYH-5	Km ^r , <i>fabG3</i> cloned into plasmid pSRK-Km	This study
pYYH-6	Km ^r , <i>XccfabG1</i> cloned into plasmid pSRK-Km	This study
pYYH-7	Km ^r , <i>E.coli fabG</i> cloned into plasmid pSRK-Km	This study
pYYH-8	Amp ^r , <i>Xcc fabG1</i> gene cloned into plasmid pBAD24M	This study
pYYH-9	Km ^r , about 1000 bp <i>Xcc xanB2</i> deletion DNA fragment inserted into pK18mobscaB between <i>EcoRI</i> / <i>HindIII</i> sites	This study
pYYH-10	Km ^r , <i>XccfabG2</i> cloned into plasmid pSRK-Km	This study

*Rif^r, Tc^r, Km^r and Amp^r indicate resistance to rifampicin, tetracycline, kanamycin and ampicillin, respectively.

inoculated in NYG medium without kanamycin at 30 °C for 36 h and then appropriate dilutions were spread onto NYG plate containing a final concentration of 10% sucrose to select the deletion mutants. Colonies sensitive to kanamycin were screened by PCR with primers *fabG3* Check Up and *fabG3* Check Down, and the *Xcc fabG3* deletion strain YH1 ($\Delta fabG3$) was obtained.

The *Xcc xanB2* deletion mutant YH8 was also obtained using a similar strategy. Moreover, the suicide plasmid pYYH-9 with the upstream and downstream fragments of *Xcc xanB2* was also transferred into the *Xcc fabG3* deletion strain YH1 and the *Xcc fabG3 xanB2* double-deletion strain YH9 was constructed.

Protein expression and purification

The pET-28b derived plasmid pYYH-3 was introduced into *E. coli* BL21 (DE3) and *Xcc FabG3* with a vector-encoded N-terminal hexahistidine (His)-tag was highly expressed (data not shown). *Xcc FabG3* was purified by nickel chelate chromatography as described previously (Yu *et al.*, 2016). The *E. coli* FabD, FabH, FabG, FabZ, FabI and holo-ACP, *V. harveyi* acyl-ACP synthetase and *R. solanacearum* RSp0194 (Mao *et al.*, 2015, 2016) were also purified as described previously (Zhu *et al.*, 2013).

Assay of *Xcc FabG3* activities *in vitro*

For the initiation reaction, the assay mixture contained 0.1 M sodium phosphate (pH 7.0), 0.1 µg each of EcFabD, EcFabH, EcFabG (or *Xcc FabG3*) and EcFabZ, 50 µM NADH, 50 µM NADPH, 1 mM β-mercaptoethanol, 100 µM malonyl-CoA, 50 µM holo-ACP and 100 µM acetyl-CoA in a final volume of 40 µL. During the long-chain 3-ketoacyl-ACP reduction, EcFabH was replaced by Rsp0194 and acetyl-CoA was replaced by octanoyl-ACP, which was synthesized from octanoic acid, ATP and holo-ACP using *V. harveyi* acyl-ACP synthetase. The assay mixtures were incubated at 37 °C for 1 h and resolved by conformation-sensitive gel electrophoresis on 20% polyacrylamide gels containing an optimized concentration of urea for separation. The gels were stained with Coomassie brilliant blue R250.

Spectrophotometric assay of OAR activity

UV-visible spectrophotometry was used to measure OAR activity through the decrease in absorbance at 340 nm, using an NADPH extinction coefficient of 6220 M⁻¹ (Qiu *et al.*, 2005). The reaction mixture contained 0.5 mM acetoacetyl-CoA, 0.2 mM NADPH, 0.1 M sodium phosphate buffer (pH 7.4) and 10 µg of a purified His-tagged *Xcc FabG1* or *Xcc FabG3* protein. When testing the enzymatic abilities of *Xcc FabG1* or *Xcc FabG3*, or cell-free extract, to reduce various 3-oxoacyl-ACP chains, the reaction mixture contained acyl-CoAs and malonyl-CoA as substrates. Additionally, 2 µg of purified *E. coli* FabD, holo-ACP and *R. solanacearum* RSp0194 were also added to the reaction mixture, in a final

volume of 100 µL. The reaction was initiated by adding 1 µg of *Xcc FabG1* or *Xcc FabG3* to the mixture, and the absorbance value was read at 340 nm.

Analysis of phospholipid compositions

The cultures were grown aerobically at 30 °C in NYG media for 2 days. Cells were harvested and washed three times with water. Fatty acid methyl esters were synthesized and extracted as described previously (Stead, 1989). Briefly, cellular lipids were saponified by the addition of 1 mL sodium hydroxide/methanol solution at 100 °C for 40 min with shaking (800 rpm). Then, fatty acids were methylated by the addition of 2 mL hydrochloric acid/methanol solution at 80 °C for 30 min and immediately cooled to below 20 °C. Fatty acid methyl esters were obtained by three extractions each with 1 mL of petroleum ether. The solvent was removed under a stream of nitrogen, and the residue was analysed by GC-MS.

Extraction and purification of DSF family signals from *Xcc* culture supernatant

The method for extraction and purification was described previously by He *et al.* (2010). To quantify DSF and BDSF production in the culture of the wild-type strain XC1 with LC-MS, 20 mL of the supernatant was collected. Its crude ethyl acetate extract was passed through a 0.45-µm Minisart filter unit and then condensed to 0.1 mL for LC-MS (Zhou *et al.*, 2015, 2015b). Two microliters of the condensed samples was applied to an AB SCIEX 6500 QTRAP system (USA) and eluted with methanol/water (80:20, v/v) at a flow rate of 0.3 mL/min in a diode array detector. BDSF and DSF levels in the culture supernatant were quantified using peak intensity (PI) in the extracted ion chromatogram.

To quantify DSF and BDSF production in the culture of strain $\Delta rpfC$ with HPLC, 50 mL of the supernatant was collected (He *et al.*, 2010). The crude ethyl acetate extract was passed through a 0.45-µm Minisart filter unit and then condensed to 0.1 mL. Then 3 µL of the extract was applied to HPLC on a C18 reverse-phase column (4.6 × 150 mm, Agilent) and eluted with water in methanol (23:77, v/v, 0.1% formic acid) at a flow rate of 1 mL/min in an Agilent Technologies 1260 Infinity system with a DAD G1315D VL detector (USA).

Quantification of xanthomonadin pigment production

Pigments were extracted from *Xcc* using previously described procedures (He *et al.*, 2011). In brief, *Xcc* cells were collected from 10 mL suspension by centrifugation and mixed with 1 mL methanol. The mixtures were then incubated for 10 min in darkness in a rotating shaker and subsequently centrifuged at 12 000 *g* for 5 min. The xanthomonadin pigments present in the supernatant were quantified using their absorbance at 445 nm.

Measurement of extracellular enzymatic activity and EPS production

Relative activities of extracellular enzymes were assayed as described previously (Chao *et al.*, 2008). Briefly, 2 μ L of each *Xcc* strain culture ($OD_{600} \approx 1.0$) was spotted onto NYG agar plates containing 1% (w/v) skim milk (for protease) (Sangon, Shanghai, China), 0.5% (w/v) carboxymethylcellulose (for cellulase) (Sangon) or 0.1% (w/v) starch (for amylase) (Sangon) and incubated at 30 °C for 24–48 h. Plates were stained where necessary. Zones of clearance around the spots due to the degradation of the substrate were photographed. Three plates were inoculated in each experiment, and each experiment was repeated three times. The relative activities of the enzymes were indicated by the diameter of the clear zones.

The EPS production was measured as described previously. Each *Xcc* strain culture (2 mL, $OD_{600} \approx 1.0$) was used to inoculate 100 mL of NYG containing 4% glucose with shaking at 180 rpm for 4 days at 30 °C. The EPS was precipitated from the culture supernatant by addition of 4 volumes of 100% ethanol. The pelleted EPS was washed with 70% ethanol, air dried and weighed. Three flasks were inoculated in each experiment and each experiment was repeated three times.

Statistical analysis

An analysis of variance for the experimental datasets was performed using JMP software v. 5.0 (SAS Institute Inc., Cary, NC, USA). Significant effects of treatment were determined by the *F* value ($P = 0.05$). When a significant *F* test was obtained, a separation of means was accomplished by Fisher's protected least significant difference at $P = 0.05$.

ACKNOWLEDGEMENTS

This work was supported by grants from the National Natural Science Foundation of China (grants 31601601 and 31671987), the National Key Project for Basic Research (grant 2015CB150600), the Natural Science Foundation of Guangdong Province (grants 2014A030313455 and 2015A030312005) and the Science Foundation of Guangdong Food & Drug Vocational College (grant 2017ZR006). The authors declare no conflict of interest.

REFERENCES

- Bi, H.K., Christensen, Q.H., Feng, Y.J., Wang, H.H. and Cronan, J.E. (2012) The *Burkholderia cenocepacia* BDSF quorum sensing fatty acid is synthesized by a bifunctional crotonase homologue having both dehydratase and thioesterase activities. *Mol. Microbiol.* **83**, 840–855.
- Bonas, U., Van den Ackerveken, G., Buttner, D., Hahn, K., Marois, E., Nennstiel, D., Noel, L., Rossier, O. and Szurek, B. (2000) How the bacterial plant pathogen *Xanthomonas campestris* pv. *vesicatoria* conquers the host. *Mol. Plant Pathol.* **1**, 73–76.
- Cao, X.Q., Wang, J.Y., Zhou, L., Chen, B., Jin, Y. and He, Y.W. (2018) Biosynthesis of the yellow xanthomonadin pigments involves an ATP-dependent 3-hydroxybenzoic acid: acyl carrier protein ligase and an unusual type II polyketide synthase pathway. *Mol. Microbiol.* **110**, 16–32.
- Chan, J.W. and Goodwin, P.H. (1999) The molecular genetics of virulence of *Xanthomonas campestris*. *Biotechnol. Adv.* **17**, 489–508.
- Chao, N.X., Wei, K., Chen, Q., Meng, Q.L., Tang, D.J., He, Y.Q., Lu, G.T., Jiang, B.L., Liang, X.X., Feng, J.X., Chen, B.S. and Tang, J.L. (2008) The *rsmA*-like gene *rsmA_{xcc}* of *Xanthomonas campestris* pv. *campestris* is involved in the control of various cellular processes, including pathogenesis. *Mol. Plant–Microbe Interact.* **21**, 411–423.
- Cheng, J.L., Ma, J.C., Lin, J.S., Fan, Z.C., Cronan, J.E. and Wang, H.H. (2012) Only one of the five *Ralstonia solanacearum* long-chain 3-ketoacyl-acyl carrier protein synthase homologues functions in fatty acid synthesis. *Appl. Environ. Microbiol.* **78**, 1563–1573.
- Dai, X.H., Gao, G., Wu, M.M., Wei, W.Y., Qu, J.M., Li, G.Q. and Ting, M. (2018) Construction and application of a *Xanthomonas campestris* CGMCC15155 strain that produces white xanthan gum. *Microbiol. Open*, e00631.
- Deng, Y.Y., Liu, X.L., Wu, J.E., Lee, J., Chen, S.H., Cheng, Y.Y., Zhang, C.Y. and Zhang, L.H. (2015) The host plant metabolite glucose is the precursor of diffusible signal factor (DSF) family signals in *Xanthomonas campestris*. *Appl. Environ. Microbiol.* **81**, 2861–2868.
- Deng, Y.Y., Wu, J.E., Yin, W.F., Li, P., Zhou, J.N., Chen, S.H., He, F., Cai, J. and Zhang, L.H. (2016) Diffusible signal factor family signals provide a fitness advantage to *Xanthomonas campestris* pv. *campestris* in interspecies competition. *Environ. Microbiol.* **18**, 1534–1545.
- Dow, J.M., Crossman, L., Findlay, K., He, Y.Q., Feng, J.X. and Tang, J.L. (2003) Biofilm dispersal in *Xanthomonas campestris* is controlled by cell-cell signaling and is required for full virulence to plants. *Proc. Natl. Acad. Sci. USA.* **100**, 10995–11000.
- Feng, S.X., Ma, J.C., Yang, J., Hu, Z., Zhu, L., Bi, H.K., Sun, Y.R. and Wang, H.H. (2015) *Ralstonia solanacearum* fatty acid composition is determined by interaction of two 3-ketoacyl-acyl carrier protein reductases encoded on separate replicons. *BMC Microbiol.* **15**, 223.
- He, Y.W. and Zhang, L.H. (2008) Quorum sensing and virulence regulation in *Xanthomonas campestris*. *FEMS Microbiol. Rev.* **32**, 842–857.
- He, Y.W., Wang, C., Zhou, L., Song, H., Dow, J.M. and Zhang, L.H. (2006) Dual signaling functions of the hybrid sensor kinase RpfC of *Xanthomonas campestris* involve either phosphorelay or receiver domain-protein interaction. *J. Biol. Chem.* **281**, 33414–33421.
- He, Y.W., Wu, J.E., Cha, J.S. and Zhang, L.H. (2010) Rice bacterial blight pathogen *Xanthomonas oryzae* pv. *oryzae* produces multiple DSF-family signals in regulation of virulence factor production. *BMC Microbiol.* **10**, 187.
- He, Y.W., Wu, J.E., Zhou, L., Yang, F., He, Y.Q., Jiang, B.L., Bai, L.Q., Xu, Y.Q., Deng, Z.X., Tang, J.L. and Zhang, L.H. (2011) *Xanthomonas campestris* diffusible factor is 3-hydroxybenzoic acid and is associated with xanthomonadin biosynthesis, cell viability, antioxidant activity, and systemic invasion. *Mol. Plant–Microbe Interact.* **24**, 948–957.
- Hu, Z., Dong, H.J., Ma, J.C., Yu, Y.H., Li, K.H., Guo, Q.Q., Zhang, C., Zhang, W.B., Cao, X.Y., Cronan, J.E. and Wang, H.H. (2018) Novel *Xanthomonas campestris* long-chain-specific 3-oxoacyl-acyl carrier protein reductase involved in diffusible signal factor synthesis. *mBio*, **9**, e00596–18.
- Khan, S.R., Gaines, J., Roop, R.M. 2nd and Farrand, S.K. (2008) Broad-host-range expression vectors with tightly regulated promoters and their use to examine the influence of TraR and TraM expression on Ti plasmid quorum sensing. *Appl. Environ. Microbiol.* **74**, 5053–5062.
- Kumar, A., Deepak, Sharma S., Srivastava, A. and Kumar, R. (2017) Synthesis of xanthan gum graft copolymer and its application for controlled release of highly water soluble levofloxacin drug in aqueous medium. *Carbohydr. Polym.* **171**, 211–219.

- Lai, C.Y. and Cronan, J.E. (2004) Isolation and characterization of beta-ketoacyl-acyl carrier protein reductase (*fabG*) mutants of *Escherichia coli* and *Salmonella enterica* serovar Typhimurium. *J. Bacteriol.* **186**, 1869–1878.
- Magnuson, K., Jackowski, S., Rock, C.O. and Cronan, J.E. (1993) Regulation of fatty acid biosynthesis in *Escherichia coli*. *Microbiol. Rev.* **57**, 522–542.
- Mao, Y.H., Ma, J.C., Li, F., Hu, Z. and Wang, H.H. (2015) *Ralstonia solanacearum* RSp0194 encodes a novel 3-keto-acyl carrier protein synthase III. *PLoS One*, **10**, e0136261.
- Mao, Y.H., Li, F., Ma, J.C., Hu, Z. and Wang, H.H. (2016) *Sinorhizobium meliloti* functionally replaces 3-oxoacyl-acyl carrier protein reductase (FabG) by overexpressing NodG during fatty acid synthesis. *Mol. Plant-Microbe Interact.* **29**, 458–467.
- Poplawsky, A.R. and Chun, W. (1997) *pigB* determines a diffusible factor needed for extracellular polysaccharide slime and xanthomonadin production in *Xanthomonas campestris* pv. *campestris*. *J. Bacteriol.* **179**, 439–444.
- Poplawsky, A.R. and Chun, W. (1998) *Xanthomonas campestris* pv. *campestris* requires a functional *pigB* for epiphytic survival and host infection. *Mol. Plant-Microbe Interact.* **11**, 466–475.
- Poplawsky, A.R., Urban, S.C. and Chun, W. (2000) Biological role of xanthomonadin pigments in *Xanthomonas campestris* pv. *campestris*. *Appl. Environ. Microbiol.* **66**, 5123–5127.
- Qian, W., Jia, Y., Ren, S.X., He, Y.Q., Feng, J.X., Lu, L.F., Sun, Q., Ying, G., Tang, D.J., Tang, H., Wu, W., Hao, P., Wang, L., Jiang, B.L., Zeng, S., Gu, W.Y., Lu, G., Rong, L., Tian, Y., Yao, Z., Fu, G., Chen, B., Fang, R., Qiang, B., Chen, Z., Zhao, G.P., Tang, J.L. and He, C.Z. (2005) Comparative and functional genomic analyses of the pathogenicity of phytopathogen *Xanthomonas campestris* pv. *campestris*. *Genome Res.* **15**, 757–767.
- Qiu, X., Choudhry, A.E., Janson, C.A., Grooms, M., Daines, R.A., Lonsdale, J.T. and Khandekar, S.S. (2005) Crystal structure and substrate specificity of the beta-ketoacyl-acyl carrier protein synthase III (FabH) from *Staphylococcus aureus*. *Protein Sci.* **14**, 2087–2094.
- Rafferty, J.B., Fisher, M., Langridge, S.J., Martindale, W., Thomas, N.C., Simon, J.W., Bithell, S., Slabas, A.R. and Rice, D.W. (1998) Crystallization of the NADP-dependent beta-keto acyl carrier protein reductase from *Escherichia coli*. *Acta Crystallogr. D. Biol. Crystallogr.* **54**, 427–429.
- Rajagopal, L., Sundari, C.S., Balasubramanian, D. and Sonti, R.V. (1997) The bacterial pigment xanthomonadin offers protection against photodamage. *FEBS Lett.* **415**, 125–128.
- Schafer, A., Tauch, A., Jager, W., Kalinowski, J., Thierbach, G. and Puhler, A. (1994) Small mobilizable multi-purpose cloning vectors derived from the *Escherichia coli* plasmids pK18 and pK19: selection of defined deletions in the chromosome of *Corynebacterium glutamicum*. *Gene*, **145**, 69–73.
- Starr, M.P. and Stephens, W.L. (1964) Pigment and taxonomy of the genus *Xanthomonas*. *J. Bacteriol.* **87**, 293–302.
- Starr, M.P., Jenkins, C.L., Bussey, L.B. and Andrewes, A.G. (1977) Chemotaxonomic significance of the xanthomonadins, novel brominated aryl-polyene pigments produced by bacteria of the genus *Xanthomonas*. *Arch. Microbiol.* **113**, 1–9.
- Stead, D.E. (1989) Grouping of *Xanthomonas campestris* pathovars of cereals and grasses by fatty acid profiling. *EPPO Bull.* **19**, 57–68.
- Ulrich, A.K., de Mendoza, D., Garwin, J.L. and Cronan, J.E. (1983) Genetic and biochemical analyses of *Escherichia coli* mutants altered in the temperature-dependent regulation of membrane lipid composition. *J. Bacteriol.* **154**, 221–230.
- Wang, L.H., He, Y., Gao, Y.F., Wu, J.E., Dong, Y.H., He, C.Z., Wang, S.X., Weng, L.X., Xu, J.L., Tay, L., Fang, R.X. and Zhang, L.H. (2004) A bacterial cell-cell communication signal with cross-kingdom structural analogues. *Mol. Microbiol.* **51**, 903–912.
- Wang, J.Y., Zhou, L., Chen, B., Sun, S., Zhang, W., Li, M., Tang, H.Z., Jiang, B.L., Tang, J.L. and He, Y.W. (2015) A functional 4-hydroxybenzoate degradation pathway in the phytopathogen *Xanthomonas campestris* is required for full pathogenicity. *Sci. Rep.* **5**, 18456.
- Yu, Y.H., Hu, Z., Dong, H.J., Ma, J.C. and Wang, H.H. (2016) *Xanthomonas campestris* FabH is required for branched-chain fatty acid and DSF-family quorum sensing signal biosynthesis. *Sci. Rep.* **6**, 32811.
- Zhou, L., Huang, T.W., Wang, J.Y., Sun, S., Chen, G., Poplawsky, A. and He, Y.W. (2013a) The rice bacterial pathogen *Xanthomonas oryzae* pv. *oryzae* produces 3-hydroxybenzoic acid and 4-hydroxybenzoic acid via XanB2 for use in xanthomonadin, ubiquinone, and exopolysaccharide biosynthesis. *Mol. Plant-Microbe Interact.* **26**, 1239–1248.
- Zhou, L., Wang, J.Y., Wang, J.H., Poplawsky, A., Lin, S.J., Zhu, B.S., Chang, C.Q., Zhou, T.L., Zhang, L.H. and He, Y.W. (2013b) The diffusible factor synthase XanB2 is a bifunctional chorismatase that links the shikimate pathway to ubiquinone and xanthomonadins biosynthetic pathways. *Mol. Microbiol.* **87**, 80–93.
- Zhou, L., Yu, Y.H., Chen, X.P., Diab, A.A., Ruan, L., He, J., Wang, H.H. and He, Y.W. (2015) The multiple DSF-family QS signals are synthesized from carbohydrate and branched-chain amino acids via the FAS elongation cycle. *Sci. Rep.* **5**, 13294.
- Zhou, L., Wang, X.Y., Sun, S., Yang, L.C., Jiang, B.L. and He, Y.W. (2015b) Identification and characterization of naturally occurring DSF-family quorum sensing signal turnover system in the phytopathogen *Xanthomonas*. *Environ. Microbiol.* **17**, 4646–4658.
- Zhou, L., Zhang, L.H., Camara, M. and He, Y.W. (2017) The DSF family of quorum sensing signals: diversity, biosynthesis, and turnover. *Trends Microbiol.* **25**, 293–303.
- Zhu, L., Bi, H.K., Ma, J.C., Hu, Z., Zhang, W.B., Cronan, J.E. and Wang, H.H. (2013) The two functional enoyl-acyl carrier protein reductases of *Enterococcus faecalis* do not mediate triclosan resistance. *mBio*, **4**, e00613–13.

SUPPORTING INFORMATION

Additional supporting information may be found in the online version of this article at the publisher's web site:

Fig. S1 (A) Strategy for isolation of *Xcc* YH1 mutant strain. (B) Genetic organization of the *fabG3* region in *Xcc* wild-type (a) or *Xcc* YH1 (b). (C) PCR analysis of genomic DNA from strains in (B). CH, chromosome; Up, upstream fragment of *Xcc fabG3*; Dn, downstream fragment of *Xcc fabG3*.

Fig. S2 (A) RT-qPCR analysis of the *fabG3* neighbouring genes *XCC4002* and *XCC4004*. (B) *Xcc* strains grown in NYG liquid medium at 30 °C. After growth, the OD₆₀₀ was monitored using the Bioscreen-C Automated Growth Curves Analysis System (OY Growth Curves FP-1100-C, Helsinki, Finland).

Fig. S3 Light absorption spectra (400–500 nm) of the pigments extracted from various *Xcc* strains.

Fig. S4 (A) The relative activity of extracellular enzymes produced by *Xcc* strains in NYG. The black columns indicate the *Xcc* wild-type strain, the grey columns indicate the mutant strain *Xcc* YH1 ($\Delta fabG3$) and the white columns indicate the complementary strain *Xcc* YH2. (B) The amount of extracellular polysaccharide (EPS) produced by the *Xcc* strains. Data are the mean \pm standard deviation of triplicate measurements. The different letters in each data column indicate significant differences at $P = 0.05$.

Fig. S5 The effects of *Xcc fabG3* deletion and expression on the production of DSF family signals and an analysis of OAR activities

in the cell-free extracts of *Xcc* $\Delta rpfC$ strains. (A) HPLC analysis of the DSF family signals extracted from different strains. (B) DSF family signals produced by *Xcc fabG3* deletion and expression strains. Supernatants of 50 mL of *Xcc* strains grown in NA medium for 36 h were collected and DSF family signals were detected by HPLC. Strain *Xcc* YH3 referred to *Xcc fabG3* gene was deleted in *Xcc* XC1($\Delta rpfC$); strain *Xcc* YH4 referred to *Xcc fabG3* complemented in plasmid pSRK-Km in *Xcc* YH3; strain *Xcc* YH5 referred to *Xcc fabG3* expressed from plasmid pSRK-Km in *Xcc* XC1($\Delta rpfC$). The relative amounts of signal molecules were calculated on the basis of their peak areas. (C) 3-oxoacyl-ACP reductase activity

analyses in the cell-free extracts of *Xcc* strains. The activities were monitored by the decrease in the absorbance at 340 nm using an NADPH extinction coefficient of 6220 m^{-1} . The reaction mixture contained octanoyl-CoA, malonyl-CoA, *E. coli* FabD, *E. coli* ACP and *R. solanacearum* RSp0194. The data shown are the means of the results of three repeats and error bars indicate standard deviations. Different letters indicate significant differences between treatments based on the least significant difference at $P = 0.05$.

Table S1 Sequences of the PCR primers used.

Table S2 Fatty acid composition of total lipid extracts from *Xcc* strain grown on NYG medium.